



Montréal, Québec  
May 29 to June 1, 2013 / 29 mai au 1 juin 2013

## Bond-Dependent Coefficient of Deformed Glass Fiber-Reinforced Polymer (GFRP) Reinforcing Bars

E. Ahmed, H.M. Mohamed, A. El-Nemr, P. Vincent, and B. Benmokrane  
Department of Civil Engineering, University of Sherbrooke, Sherbrooke, Quebec, Canada

**Abstract:** Concrete members reinforced with glass fiber-reinforced polymer (GFRP) bars exhibit large crack widths and deflections in comparison with that reinforced with steel bars due to the low modulus of elasticity of GFRP bars. Consequently, the design of GFRP-reinforced concrete (GFRP-RC) members is often governed by serviceability (deflection and cracking) rather than ultimate state. The calculation of the crack width, however, includes an important parameter to account for the bond between the FRP bars and the surrounding concrete which is the bond-dependent coefficient ( $k_b$ ). This paper presents the test results of an investigation conducted to evaluate the bond bond-dependent coefficient ( $k_b$ ) of newly developed helically-deformed GFRP bar. A total of 4 concrete beams ( $200 \times 300 \times 3100$  mm) were constructed and tested in four-point bending in accordance with the new test method presented in Annex S of CSA S806-12 “*Test Method for Determining the Bond-Dependent Coefficient of FRP Rods*”. The investigation included four different diameters of the deformed GFRP bars, namely: 12, 16, 20, and 25 mm. The predicted  $k_b$  values were compared with the recommendation of ACI 440.1R-06 design guidelines and the CSA S6-06 Code. The average  $k_b$  value of the newly developed helically-deformed GFRP bars is 0.90. In addition, the  $k_b$  value provided by ACI 440.1R-06 overestimated the crack widths of these bars in concrete beam while that of CSA S6-06 was close to the predicted ones.

### 1 Introduction

Bond characteristic of fiber-reinforced polymer (FRP) bar is one of the most important parameters that control the design of FRP-reinforced concrete (FRP-RC) members. Concrete members reinforced with glass FRP (GFRP) bars exhibit larger crack widths and deflections in comparison with that reinforced with steel bars, as a result of the low modulus of elasticity of GFRP bars (Benmokrane et al. 1995; ACI 440 2006). Consequently, in many cases, serviceability requirements (crack width and deflection) govern the design of such members rather than ultimate limit state requirements. The calculations of the crack width of the FRP-RC members include the bond-dependent coefficient ( $k_b$ ) to account for the bond between the FRP bars and the surrounding concrete. Therefore,  $k_b$  is one of the most important parameters that affect the design of concrete members reinforced with GFRP bars.

The recently published CSA S806 (2012) provides a test method to experimentally determine  $k_b$  values “*Test Method for Determining the Bond-Dependent Coefficient of FRP Rods*”. In addition, the current available design codes and guides provide recommended values for the  $k_b$  that should be verified from the tests if needed. CSA S6 (2010) states that  $k_b$  shall be determined experimentally but in the absence of test data it can be taken as 0.8 for sand-coated FRP bars and 1.0 for deformed FRP bars. ACI 440 (2006) reports that the average  $k_b$  values range from 0.60 to 1.72 with an average 1.10. Thus, there may be a need to evaluate the  $k_b$  values for any of the FRP bars prior to using them in design and applications.

This paper presents an experimental investigation to evaluate the bond-dependent coefficient ( $k_b$ ) of newly developed helically-deformed GFRP bar and compare it with the recommendations of the current FRP design codes and guides. The tests were conducted in accordance with Annex S “*Test Method for Determining the Bond-Dependent Coefficient of Fibre-Reinforced Polymer (FRP) Rods*” of CSA S806 (2012).

## 2 Experimental Work

### 2.1 Materials

#### 2.1.1 Concrete

The beam specimens were constructed using normal strength concrete with target compressive strength of 35 MPa. The concrete was provided by a local ready-mix concrete supplier. The maximum size of the coarse aggregates was 20 mm. Six concrete cylinders (150 x 300 mm) were prepared and cured under the same conditions as the test specimens. Three cylinders were tested in compression at the day of test and the average concrete compressive strength was equal to  $41.5 \pm 3.6$  MPa. The remaining three cylinders were tested in splitting tension test and the average tensile strength ranged from 3.6 to 3.9 MPa.

#### 2.1.2 GFRP bars

New developed helically-deformed GFRP bars, shown in Figure 1, were used. Four different diameters of these GFRP bar were used in concrete beams. The used diameters were 12, 16, 20, and 25 mm. The tensile properties of the GFRP bars were determined by performing tensile tests on representative specimens in accordance with CSA S807 (2010) and CSA S806 (2012). Table 2 presents the mechanical properties of the GFRP bars determined from testing.



Figure 1: GFRP reinforcing bars

Table 1: Properties of the deformed GFRP bars

Bar diameter (mm)	Cross-sectional area (mm <sup>2</sup> )	Tensile strength (MPa)	Tensile modulus (GPa)	Strain at failure (%)
12	113	1166 ± 39	65 ± 3	1.8 ± 0.1
16	201	1122 ± 51	63 ± 2	1.8 ± 0.1
20	314	1117 ± 65	69 ± 3	1.6 ± 0.1
25	490	1340 ± 68	65 ± 2	2.0 ± 0.1

### 2.2 Test specimens

A total of four reinforced concrete beams were constructed and tested up to failure. The tested beams measured 3100 mm long, 200 mm wide, and 300 mm deep as shown in Figure 2. The beams had a 200 mm overhang length beyond the supports on each side as anchorage length to avoid bond failure. The shear span was kept constant at 1100 mm for all beams. The beam specimens were provided with 10M stirrups in the shear spans to avoid shear failure. The beams were fabricated using normal-strength

concrete with a compressive strength of  $41.5 \pm 3.6$  MPa. Each specimen was reinforced longitudinally with 2 10M steel bars as top reinforcement and 2 GFRP bars of 12, 16, 20, and 25 mm diameter as bottom reinforcement with corresponding GFRP reinforcement ratios ( $\rho$ ) of 0.43, 0.77, 1.25, and 1.96%. As required by the Annex S of the CSA S806 (2012) the clear cover in case of 12 and 16 mm-diameter GFRP bars was 38 mm whereas the clear cover was 50 mm for GFRP bars of 20 and 25 mm-diameters. Figure 2 shows the reinforcement details of the beam specimens while Table 2 presents the details of each beam. Figure 3 shows the fabrication of the test specimens.

Table 2: Test matrix and reinforcement details

Beam <sup>a</sup>	$f_c$ (MPa)	Bottom longitudinal reinforcement	Top longitudinal reinforcement	Area of bottom reinforcement (mm <sup>2</sup> )	Reinforcement ratio (%)
N2#4	41.5±3.6	2 - 12 mm	2 - 10M steel	226	0.43
N2#5		2 - 16 mm	2 - 10M steel	402	0.77
N2#6		2 - 20 mm	2 - 10M steel	628	1.25
N2#8		2 - 25 mm	2 - 10M steel	980	1.96

<sup>a</sup> N denotes normal-strength concrete, followed by number and diameter of GFRP bars.

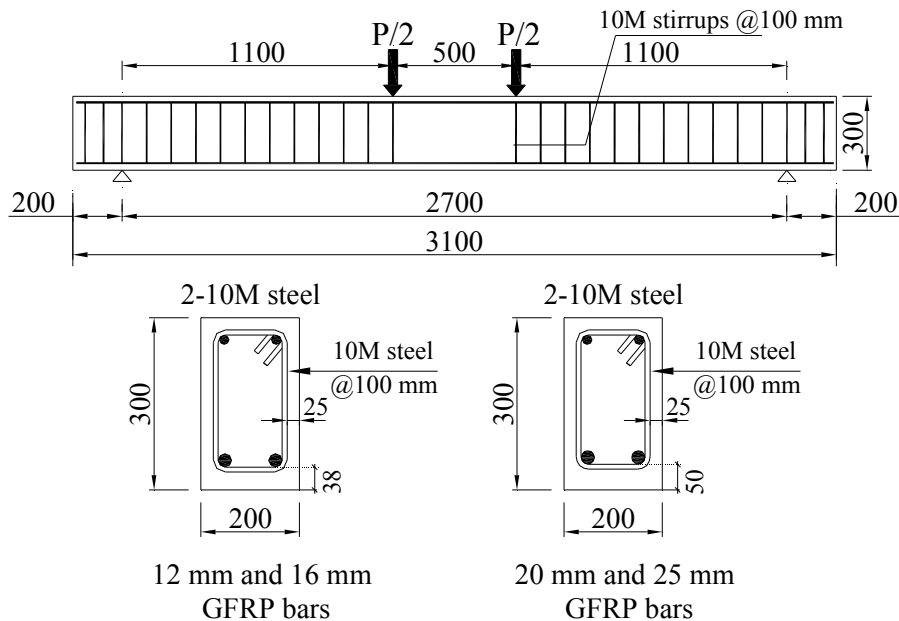


Figure 2: Dimensions and reinforcement details of the beam specimens



Figure 3: Fabrication of beam specimens

### 2.3 Instrumentation and test setup

Electrical-resistance strain gauges were used to measure the tensile strains in the GFRP reinforcing bars and the compressive strains in the concrete beams at the desired locations. These gauges were glued on several locations as shown in Figure 4. Four electrical strain gauges (6 mm) were glued on the longitudinal reinforcing bars at the middle of the beam and under the loading points. In addition, two electrical strain gauges (60 mm) were glued on the top surface of the concrete beams at mid-span to measure the concrete compressive strains. The deflection of each beam was measured using four LVDTs at the mid-span and under the loading points. Three high-accuracy LVDTs ( $\pm 0.001$  mm) were used to measure the width of the first three flexural cracks in the constant moment zone.

The specimens were tested in four-point bending over a simply-supported clear span of 2700 mm. The load was applied using a 500 kN closed-loop MTS actuator with a stroke-controlled rate of 1.2 mm/min. The loading was stopped when the first three flexural cracks appeared and the initial crack widths were measured manually using a hand-held 50X microscope. Thereafter, the LVDTs were installed to continuously monitor the crack widths with the load increase. The MTS actuator, strain gauges and LVDTs were connected by a Data Acquisition System and the data were recorded every second during the test. During the test the crack propagation was marked on the beam and the corresponding loads were recorded. Figure 5 shows the test setup during a beam test.

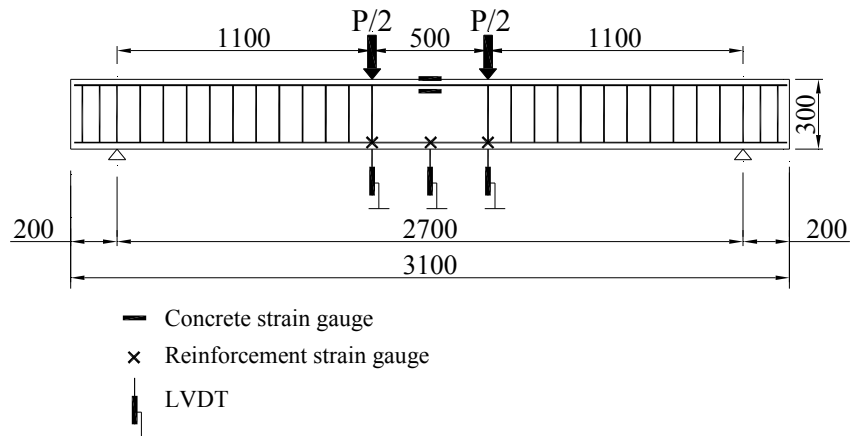


Figure 4: Schematic of beam instrumentation

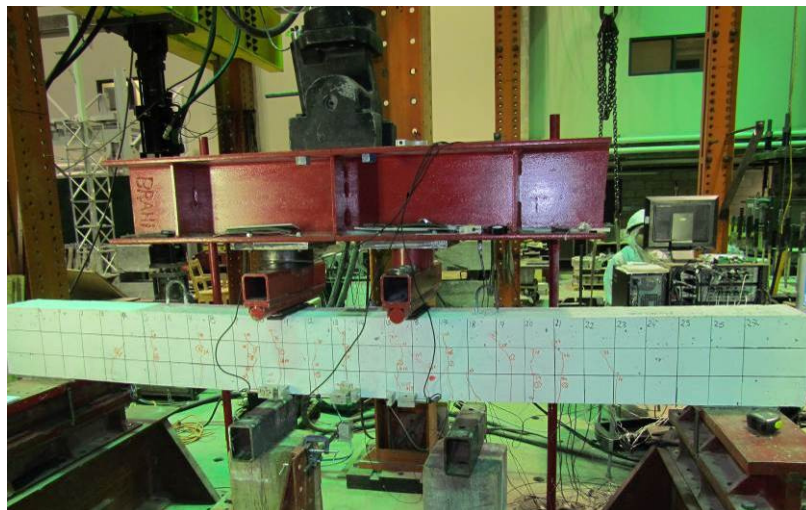


Figure 5: Overview of the test setup

### 3 Experimental Test Results

#### 3.1 Crack pattern and mode of failure

The four tested beams failed in compression due to concrete crushing as they were over-reinforced. The crack patterns and mode of failure are shown in Figure 6. Similar crack patterns were observed for the four beams. Crack formation was initiated in the constant moment flexural zone between the two concentrated loads. The cracks were vertical perpendicular to the direction of the maximum principle tensile stress induced by pure bending. The cracking load ranged between 14.5 and 18.14 kN for the tested beam specimens. These values are approximately 11 to 15% of the ultimate load. As load increased, additional flexural cracks appeared and the crack spacing decreased. It can be noticed from these crack patterns that the beams have almost the same number of cracks in the constant flexural moment zone. Finally, the beams failed due to crushing of the concrete at the top surface (compression side) between the two concentrated loads. Figure 6 shows the beam specimens at failure.

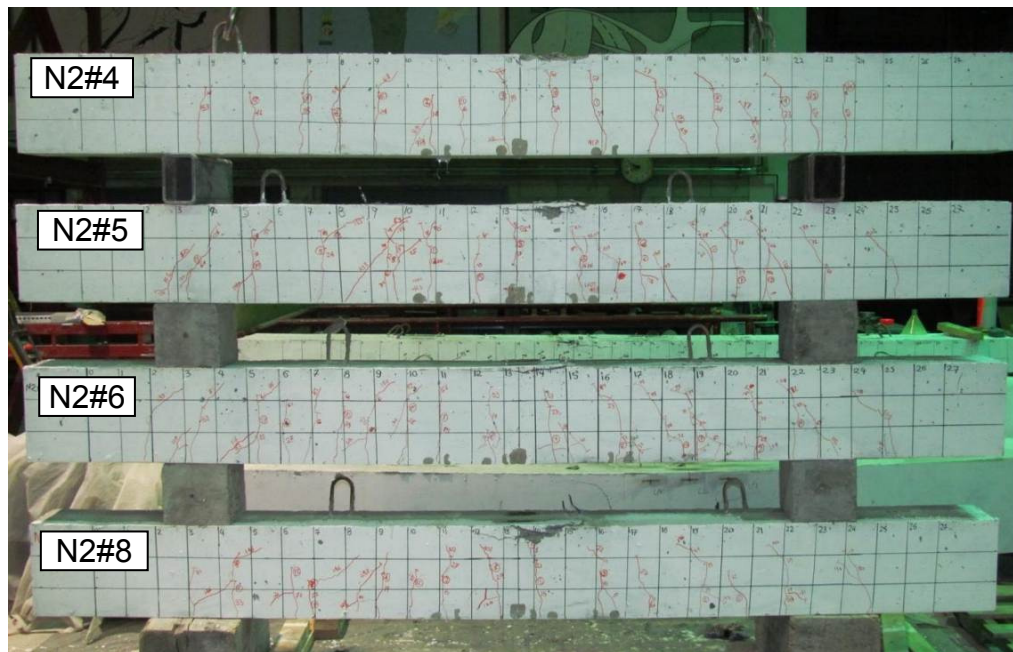


Figure 6: Crack pattern at failure of the tested beams

#### 3.2 Reinforcement and concrete strains

Figure 7 shows the measured mid-span tensile strains in the GFRP bars as well as the mid-span concrete strains versus the applied load for the tested beams. Generally, all the beams exhibited typical bi-linear load strain relationships and the higher the reinforcement ratio, the lower the concrete and GFRP bar strains at the same load level. The maximum measured compressive strains in the concrete were 2490, 2780, 3112, and 3300 microstrains for N2#4, N2#5, N2#6 and N2#8 beams, respectively. On the other hand, the maximum measured tensile strains in the GFRP bars ranged from 8100 to 11200 microstrains. These values approximately represent 45 to 55% of the ultimate tensile strain of the GFRP bars obtained from the standard tensile tests (see Table 1). This confirms the compression failure of the tested GFRP-RC beams.

The measured strains in the GFRP reinforcing bars are used to evaluate the bond-dependent coefficient ( $k_b$ ). The stress in GFRP reinforcement in tension ( $f_f$ ) was calculated as strain  $\times$  tensile modulus of elastic of the GFRP bars. The calculations were made at 30% of the nominal capacity ( $0.3M_n$ ) of the test specimens as this value was reported as the service load level by many researchers (Mota et al. 2006; Bischoff 2009; El-Nemr et al. 2011).

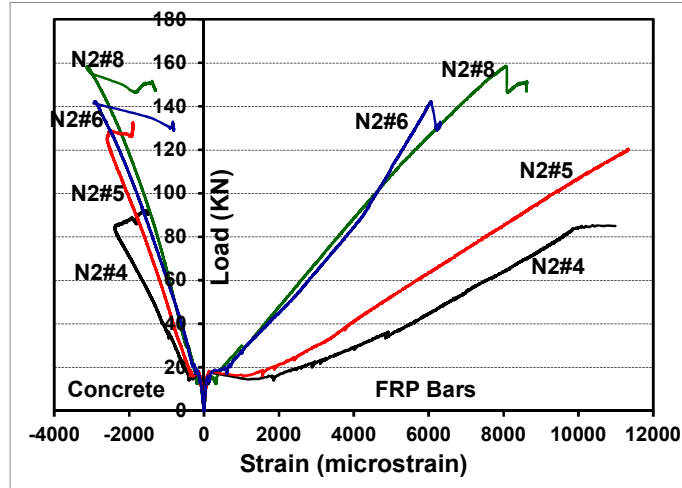


Figure 7: Load-flexural compression and tension relationships

#### 4 Prediction of Bond-Dependent Coefficient ( $k_b$ )

According to CSA S806 (2012), Annex S, the bond-dependent coefficient ( $k_b$ ) should be determined from the measured crack widths and strains in the FRP bars (at service stage) during testing and using Eq. (1) (ACI 440 2006; CSA S6 2010).

$$[1] \quad w = 2 \frac{f_f}{E_f} \beta \times k_b \times \sqrt{d_c^2 + \left(\frac{s}{2}\right)^2}$$

where  $w$  is the maximum crack width (mm),  $E_f$  is the modulus of elasticity of FRP bar (MPa),  $f_f$  is the stress in FRP reinforcement in tension (MPa),  $k_b$  is the bond dependent coefficient,  $\beta$  is the ratio of distance from neutral axis to extreme tension fibre to distance from neutral axis to centre of tensile reinforcement,  $d_c$  is the thickness of concrete cover measured from extreme tension fibre to centre of bar (mm), and  $s$  is the longitudinal FRP bar spacing (mm).

It should be mentioned that the design codes and guides provide different values for  $k_b$  depending on the surface configurations of the FRP bars. Table 3 summarizes the recommended values by ACI 440 (2006) and CSA S6 (2010).

Table 3: Design recommendations for  $k_b$  values of design codes and guides

ACI 440 (2006)	CSA S6 (2010)
$k_b$ values ranging from 0.60 to 1.72 (mean of 1.10)	Sand-coated FRP: $k_b = 0.8$
Conservative value of $k_b = 1.4$ (excluding smooth bars and grids)	Deformed FRP: $k_b = 1.0$

##### 4.1 Crack width comparisons and $k_b$ evaluation

Figure 8 shows the measured crack widths in the tested beams. Figure 8 also shows comparison with predicted crack widths using the recommended bond-dependent coefficients ( $k_b$ ) of ACI 440 (2006) and CSA S6 (2010) provided in Table 3. The ACI 440 (2006) states that  $k_b$  can vary from 0.60 to 1.72, and a design value of 1.40 can be assumed if bond is not known while CSA S6 (2010) recommends a  $k_b=1.0$  for deformed FRP bars. The comparison in Figure 8 shows that the  $k_b=1.4$  of ACI 440 (2006) is very conservative and overestimates the crack widths in the tested beams. On the other hand, the  $k_b=1.0$  provided by CSA S6 (2010) yields crack widths close to the measured ones in the tested beams.

The bond-dependent coefficient ( $k_b$ ) was calculated from the measured cracks and strains in the tested beams. Once again, the calculations were made at 30% of the nominal capacity ( $0.3M_n$ ) of the tested specimens as this value was reported as the service load level by many researchers (Mota et al. 2006; Bischoff 2009; El-Nemr et al. 2011). Table 4 provides the calculated  $k_b$  values. The calculated  $k_b$  values ranged from 0.71 to 1.03 with an average of  $0.90 \pm 0.14$ .

Table 4: Calculated  $k_b$  values of the deformed GFRP bars at  $0.3M_n$

Beam	Calculated $k_b$ values			Average
	Crack #1	Crack #2	Crack #3	
N2#4	0.85	1.10	--	0.98
N2#5	0.75	0.72	0.65	0.71
N2#6	1.16	--	0.91	1.03
N2#8	0.78	0.91	0.95	0.88
Overall average				0.90
Standard deviation				0.14

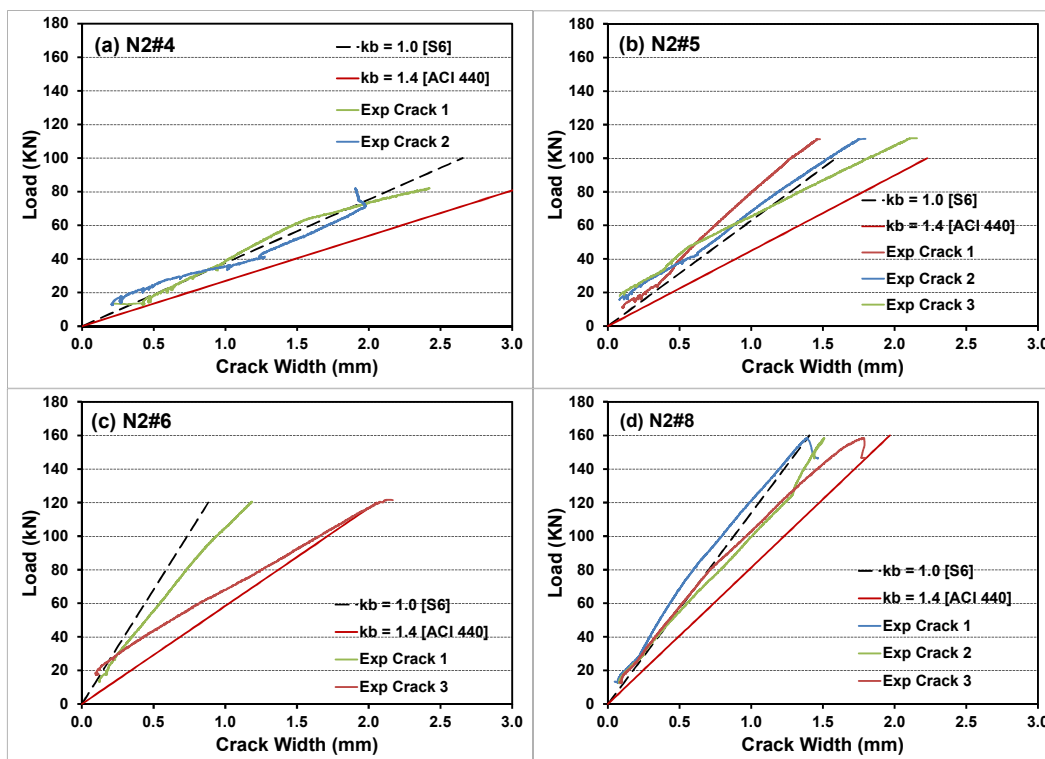


Figure 8: Measured and predicted crack widths of the tested beams

## 5 Conclusions

This paper presents the test results of an investigation conducted to evaluate the bond bond-dependent coefficient ( $k_b$ ) of newly developed helically-deformed GFRP bar. A total of 4 full-scale concrete beams ( $200 \times 300 \times 3100$  mm) were constructed and tested in four-point bending in accordance with the new test method presented in Annex S of CSA S806-12 "Test Method for Determining the Bond-Dependent Coefficient of FRP Rods". Based on the test results and the discussions, the following conclusion can be drawn:

1. In most cases, there is no major difference between the crack widths measured in the same beam in the flexural zone. Consequently, the bond-dependent coefficient ( $k_b$ ) calculated from many cracks in the flexural zone in the same beam may be of close values.
2. The calculated bond-dependent coefficient ( $k_b$ ) ranged from 0.71 to 1.03 with an average of  $0.90 \pm 0.14$ . This values is close to the  $k_b=1.0$  provided by CSA S6 (2010) for deformed FRP bars.
3. The crack-width prediction of CSA S6 (2010) was very close to the measured crack widths in the tested beams while ACI 440 (2006) overestimated the crack widths because of the higher  $k_b$  values provided by ACI 440 (2006).

## 6 Acknowledgments

The authors would like to express their special thanks and gratitude to the Natural Science and Engineering Research Council of Canada (NSERC), the Fonds quebécois de la recherche sur la nature et les technologies (FQRNT), the Canadian Foundation for Innovation (FCI), and the technical staff of the structural lab of the Department of Civil Engineering at the University of Sherbrooke.

## 7 References

- ACI Committee 440. 2006. Guide for the Design and Construction of Concrete Reinforced with FRP Bars. ACI 440.1R-06, American Concrete Institute, Farmington Hills, Mich., 44 p.
- Benmokrane, B., Chaallal, O., and Masmoudi, R. 1995. Flexural Response of Concrete Beams Reinforced with FRP Reinforcing Bars. *ACI Structural Journal*, 91(2): 46–55.
- Bischoff, P.H., Gross, S., and Ospina, C.E. 2009. The Story behind Proposed Changes to the ACI 440 Deflection Requirements for FRP-Reinforced Concrete. ACI SP-264, *American Concrete Institute*, eds. Ospina, C., Bischoff, P., and Alkhrdaji, T., MI, pp. 53-76.
- Canadian Standard Association (CSA), 2010. Canadian Highway Bridge Design Code. CAN/CSA S6-06, Addendum, Rexdale, Ontario, Canada.
- Canadian Standard Association (CSA). 2010. Specification for Fibre-Reinforced Polymers. CAN/CSA S807-10, Rexdale, ON, Canada, 27 p.
- Canadian Standard Association (CSA). 2012. Design and Construction of Building Structures with Fibre Reinforced Polymers. CAN/CSA S806-12, Canadian Standards Association, Rexdale, ON, Canada.
- El-Nemr, A., Ahmed, E., and Benmokrane, B. 2011. Instantaneous Deflection of Slender Concrete Beams Reinforced with GFRP Bars. *Proceedings of the 2<sup>nd</sup> International Engineering Mechanics and Materials Specialty Conference*, CSCE, Ottawa, Ontario, June 14-17, (CD-ROM), 10 p.
- Mota, C., Alminar, S., and Svecova, D. 2006. Critical Review of Deflection Formulas for FRP-RC Members. *ASCE Journal of Composites for Construction*, 3(10): 183-194.